Nuclear Inst. and Methods in Physics Research B xxx (xxxx) xxx–xxx

Contents lists available at ScienceDirect

Nuclear Inst. and Methods in Physics Research B

journal homepage: www.elsevier.com/locate/nimb

Studies of systematic effects of the AstroBox2 detector in online conditions

A. Saastamoinen[a,*], E. Pollacco[b], B.T. Roeder[a], R. Chyzh[a], L. Trache[c], R.E. Tribble[a]

[a] Cyclotron Institute, Texas A&M University, College Station TX-77843, USA
[b] IRFU, CEA, Universite Paris-Saclay, F-91191 Gif-sur-Yvette, France
[c] National Institute of Physics and Nuclear Engineering, Bucharest-Magurele RO-077125, Romania

ARTICLE INFO

Keywords:
Radioactive ion beams
Micro pattern gas amplifier detector
Micromegas
Implantation
$\beta p \beta \alpha$

ABSTRACT

After commissioning the AstroBox2 detector has been used already for several physics experiments. During some of the experiments systematic effects in the measured decay spectra have been observed and related to gain shifts due to the environment, the chemical nature of the isotope under investigation, and to the beam implantation rate. In this article we report the observations and influence of these systematic effects that may well be of interest to other similar experiments with stopped rare isotope beams and detectors relying on gas amplification. Full characterization and understanding of these effects call for further systematic studies.

1. Introduction

The AstroBox2 detector [1] is a gas-filled calorimetric detector which is optimized for almost background free low-energy β-delayed charged particle spectroscopy. It is an upgraded version of the original AstroBox [2] proof-of-concept detector based on Micromegas (MICRO MEsh GAseous Structure) technology [3]. After the initial commissioning described in [1] some extensive upgrades have been made in conjunction with the first physics experiments. A new gating grid covering the whole detector has been built and instrumented with a dedicated fast HV switch. The setup has been instrumented further with two different high-purity Ge detector setups for particle-delayed γ detection. While developing the detector extensive offline measurements were made to understand the behavior of different components. We report here on observations of systematic effects that can have influence on the online data obtained with gas-filled detectors.

2. Online results from β-delayed particle decays of ^{20}Na, ^{23}Al, ^{25}Si, ^{31}Cl, ^{32}Cl, and ^{35}K

All the experiments were conducted at the Cyclotron Institute of Texas A&M University. The rare isotope beams of ^{20}Na, ^{23}Al, ^{25}Si, ^{31}Cl, ^{32}Cl, and ^{35}K were produced either through fragmentation or fusion evaporation reactions at an energy range of 36–45 MeV/u, depending on the case. The reaction products were separated with the Momentum Achromat Recoil Spectrometer (MARS) [4] and implanted inside the AstroBox2 detector by adjusting a rotatable Al degrader. All experiments were run in pulsed mode such that the beam implant/measure cycle was about twice the half-life for each isotope, respectively. In each experiment, the gas was ultra-high purity P5 (Ar:CH_4 95%:5%, grade 5.0) at 800 Torr and an ambient temperature typically at 300 K. The drift field was kept constant at 216.4(15) V/cm and the typical amplification field used was ~30 kV/cm. The dynamic range of the detector (combination of electronic and gas gain) was set to about 1.5 MeV full scale for a 8 k ADC, TDC signals were recorded with 800 ps resolution, and events were timestamped with a 10 kHz clock.

2.1. Gain shifts

Gas gain, especially in the exponential regime of a Micromegas, can be very sensitive to various changes in the detection medium such as gas impurity levels and gas density changes due to either pressure or temperature fluctuations. The typical requirement of reaching $\lesssim 1-10$ ppm impurity level for H_2O and O_2 can be achieved by using commercially available high-purity gases and by proper detector design and preparation and handling of the system itself. The AstroBox2 gas handling uses an MKS piPC99 mass flow controller which ensures stable pressure conditions (manufacturer claims accuracy ±1.0%). Given the stable pressure, possible environment temperature variations may induce gain shifts. However, in the experimental cave which remains closed during the beam time, the temperature stabilizes during beam tuning and is monitored during experiments. To track possible gain drift we have implemented multiple independent ways to monitor the stability of the detector: (i) an α source on an active side pad of the detector, (ii) a separate chamber for a 1 cm^2 Micromegas detector using ^{55}Fe X-ray source at the gas exhaust, (iii), a pulser in the AstroBox

* Corresponding author.
E-mail address: ajsaasta@comp.tamu.edu (A. Saastamoinen).

https://doi.org/10.1016/j.nimb.2019.05.026
Received 1 February 2019; Received in revised form 2 April 2019; Accepted 9 May 2019

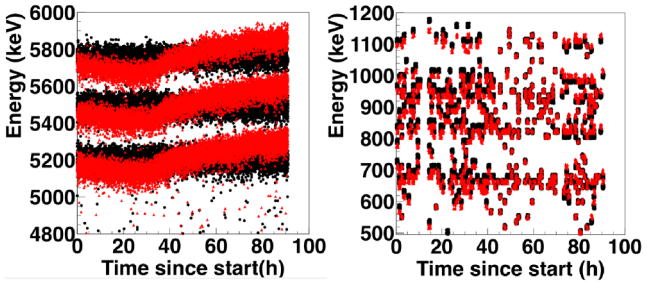

Fig. 1. Black solid dots: Calibrated data without gain shift corrections. Red triangles: Calibrated data corrected with gain shift correction on an hourly basis. Left panel shows ^{239}Pu, ^{241}Am, ^{244}Cm peaks from the mixed source data collected during the beam time. The right panel shows the ^{35}K decay data collected during this period. The observed gain shift can be attributed to gas bottle running out and change to a new bottle about a day after the start of the experiment. See text for more details. (For interpretation of the references to colour in this figure legend, the reader is referred to the web version of this article.)

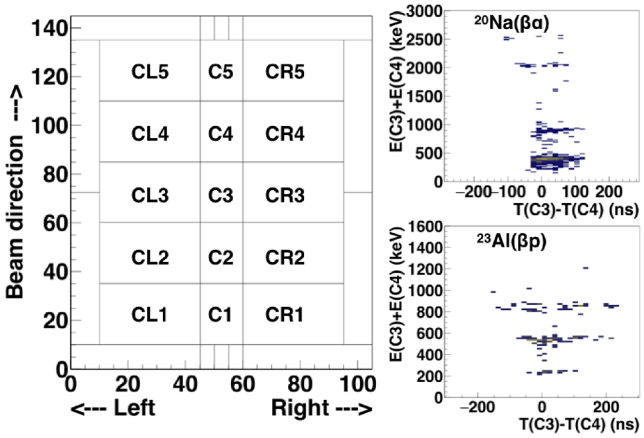

Fig. 2. Left: The pad layout with labels for the pads in the central region used in analysis. Units denote dimensions in mm. Right: The total decay energy collected with two neighboring pads from the central region (labeled C3 and C4) versus the time difference of the same pads in case of ^{20}Na and ^{23}Al measured with AstroBox2. Here the positive time difference in pad drift times corresponds to particle trajectory towards the anode and the negative time difference to a trajectory towards the cathode. The spectra are produced from beam off period with requirement of exactly two pads firing, and that the maximum energy deposition of the event is not on the pad where decay occurred. See text for more details.

electronics, and (iv) possible strong decay branches of the species under study. In most cases when the environment is under control, no gain shifts beyond the typical instrument resolution are observed.

Fig. 1 illustrates an example from an experiment where the beam time had to be started with an old gas bottle and the fresh replacement arrived only after the experiment had started. It is clear that towards the end of the old bottle during the first day and half there is an observable drop in gain. To keep all the operating voltages on and to avoid relatively a long venting and pumping process of the detector with the fragile beam window, only the gas lines were purged when changing the bottle. It is evident that with the gas throughput used it took several days for the gain to return to the baseline. This effect was replicated after the experiment in offline conditions. The origin of this effect can be attributed to the higher impurity concentration towards the end of the gas bottle as colloquially observed in operation of other types of gas detectors and devices such as gas cells.

The gain shifts is corrected by utilizing the simultaneously collected α source data from an active side pad. Fig. 1 illustrates the gain shift corrected data (red solid triangles) overlaid with the data without corrections (black solid dots). Here, the collected α source data is evaluated on an hourly basis and if a change to the baseline (first hour of the ^{25}Si calibration run in very beginning of the beam time) is observed, a linear normalization to the baseline was applied. The source strength allows corrections even at shorter time intervals if needed, but shorter than an hour is not observed to improve the data beyond the instrument resolution.

2.2. Drifting of stopped beam species

Within the present operating pressures and temperatures the implanted ions if rapidly neutralized will exercise a Brownian motion and will be localized within a sphere of few mm of the stopping position at decay. This will yield a detection efficiency of close to 100%. However for relatively low electron affinities with respect to the P5 constituents, the ions (with possibly additional molecular aggregation) will drift towards the cathode. In this case the efficiency will vary to reach close to 50% when ions are stopped in the cathode. The latter leads to a varying detection efficiency along the ion trajectory depending on a number of uncontrolled factors. Further the detected charge will in turn depend on the recoil mass or backing. Hence a distorted resolution.

In the 1990's Blank et al. studied the possibility of stopping rare isotopes inside of a gaseous microstrip detector and collecting the surviving ions on the cathode with a Si detector and reported 80% of ^{20}Na and 15% of ^{21}Mg being collected on the Si detector [5]. It is known that typical ion mobilities, μ, in low concentration Ar + CH_4 mixtures ($CH_4 \lesssim 20\%$) in low drift fields are around 1.5...1.8 $cm^2V^{-1}s^{-1}$ [6]. Therefore under the typical operating conditions of AstroBox2 the ion drift time from the beam axis, along which the beam is stopped, to the cathode is in order of several tens of milliseconds, depending on the element (e.g. $t_{drift}(Ar^+) \approx 19$ ms).

Fig. 2 shows examples of the total decay energy collected with two neighboring pads from the central region (labeled C3 and C4, location on the detector shown in the left panel of Fig. 2) versus the time difference of the same pads in cases of deposited ions ^{20}Na and ^{23}Al. The positive time difference in drift times corresponds to particle trajectory towards the anode and the negative time difference to a trajectory towards the cathode. The spectra are produced from the beam off period with requirement of exactly two pads firing in the decay event. Furthermore, to identify where the decay originated, one can require that the maximum energy deposition of the event is not on the centermost pad (C3) of the detector. The most notable feature is in the case of $\beta\alpha$-decay of ^{20}Na where both the α's and ^{16}O recoils are observed separately. In a gas-based calorimeter this is possible only when the decay occurs on a surface such as the cathode. Moreover, the drift time differences are on the positive side, implying that the particle tracks have been drifting exclusively towards the anode. The few events with negative drift time differences are likely decays over the interface between the pads, fulfilling the required gating conditions. The limited data implies 65(20)% of ^{20}Na ending on cathode in agreement with Ref. [5]. In the βp-decay of ^{23}Al there is some imbalance for decays towards the anode, but more statistics are needed to quantify the effect. In cases of βp-decays of ^{25}Si, ^{31}Cl, and ^{32}Cl (also $\beta\alpha$) there is no preferred direction and therefore all decays occur inside the gas volume. The βp-decay of ^{35}K show some imbalance between positive and negative drift time differences implying a mixture of decays both in gas and on the cathode. Based on these observations it seems that group 1 elements Na and K survive in ion form even in noble gas hydrocarbon mixture while other elements studied are neutralized before reaching the cathode. These observations are in agreement with findings of Blank et al. [5], but would require a more dedicated systematic study to be fully characterized.

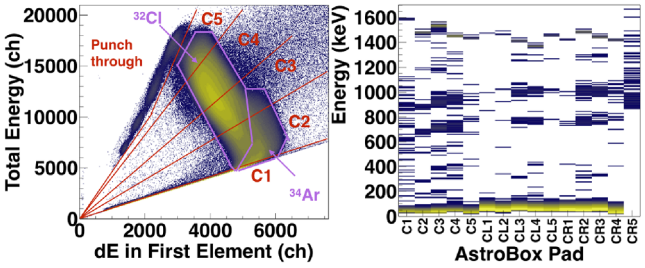

Fig. 3. Left: The total energy deposition of the central pads (C1-C5) versus the energy loss in the first pad (C1) during beam on phase of ^{32}Cl experiment. The implantation distribution of ^{32}Cl is centered over pads C3 and C4 with tails over to the other pads. Strong ^{34}Ar contamination is stopped mostly before the active pads, but with tail expanding to pads C1 and C2. Right: The summarized $M = 1$ decay spectra of ^{32}Cl from each pad from the center region (C1-C5) and the neighboring pads from the left (CL1-CL5) and the right (CR1-CR5) side. A visible drop in gain (down to ~80% on pad C1) is seen towards the beginning of the detector. See text for more details and right panel of Fig. 2 for the pad layout.

2.3. Implantation and decay rate related effects

Gas detectors in general are known to have ionization rate dependent gain losses. Micromegas based gas amplifiers are known to tolerate particle fluxes up to 10^9mm^{-2}s^{-1}, but this depends strongly on type of particles detected and gas mixture used [7]. In the AstroBox experiments, when everything is under control, we have not observed any rate related effects up to about kHz total implant/decay rates. However, here we present a curious rate related effect from an experiment where a non-standard gas handling system had to be used (the standard gas system was in service). The unknown chemical history of the spare gas system is the likely cause for the following effects to appear even at low ionization rates.

The left panel of Fig. 3 shows the beam implantation distribution in the central region of the detector from the beam on phase of ^{32}Cl experiment and the right panel shows the summarized $M = 1$ gated β-delayed particle spectra of ^{32}Cl from each pad from the active region during the beam off period. A visible drop in the peak positions of the strongest 762 and 996 keV proton groups, as well as in the extent of the β-background, is observed towards the beginning of the central region of the detector (pads C1-C3). For example in the case of pad C1 (the first pad in the entrance) the overall pulse height drops down to about 80% of the nominal value. Remarkably, the pulse height remains stable at the calibrated value on the side pads where fewer ions are implanted during the beam on period. Since this effect is localized over certain pads, and is not uniformly across the whole detector, it is likely not related to the mesh which is shorted to ground ($R = 0\Omega$). Notably, this effect is observed during the decay phase when the ionization effects from the beam implantation phase should be already terminated: even at highest the plasma density remains relatively low ($\lesssim 10^6$ ion-electron pairs/cm^3 per stopped particle). As the electrons are collected in μs and the ions drift to the cathode in 10^1 ms time scale, the beam related ionization should not interfere with the decay measurement (beam off) phase. Therefore, this observed effect originates likely from β-decays since the βp-branching ratios are order of few 10^{-4} in case of ^{32}Cl (total β-activity per pad up to kHz). It is one possibility that the flux of β's inside the detector leads to extra ionization throughout the active volume causing some of the primary ionization electrons from the proton track to recombine with free ions before being able to drift towards the mesh and amplification gap.

3. Conclusions and outlook

During some (but not all) of our experiments with low energy β-delayed particle emitters we have observed systematic effects in the measured β-delayed particle spectra and related these to gain shifts due to changes in the environment, the chemical nature of the isotope under investigation, and to the beam implantation rate (or the decay ionization rate). Full characterization and understanding of these effects call for further systematic studies. Meanwhile in these kind of experiments a careful operation of the system followed by a case by case analysis accompanied by full simulations of the detector are required to fully understand the observed decay spectra.

Acknowledgements

This work has been supported in part by the US DOE under Grants DE-FG02-93ER40773 and DE-NA0001786. The authors thank Rui De Oliviera and Bertrand Mehl CERN (EP-DT) for their assistance in developing the MPGD for the project.

References

[1] A. Saastamoinen, et al., Nucl. Instrum. Meth. Phys. Res. B 376 (2016) 357.
[2] E. Pollacco, et al., Nucl. Instrum. Meth. in Phys. Res. A 723 (2013) 102.
[3] Y. Giomataris, et al., Nucl. Instrum. Meth. in Phys. Res. A 376 (1) (1996) 29.
[4] R. Tribble, et al., Nucl. Phys. A 701 (2002) 278.
[5] B. Blank, et al., Nucl. Instrum. Meth. Phys. Res. A 330 (1) (1993) 83.
[6] W. Blum, W. Riegler, L. Rolandi, Particle Detection with Drift Chambers, second ed., Springer, Berlin/ Heidelberg, 2008.
[7] G. Charpak, et al., Nucl. Instrum. Meth. Phys. Res. A 478 (2002) 26.